

Cryoelectron Tomography: Implications for Actin Cytoskeleton Research*

Igor Weber

*Ruđer Bošković Institute, Department of Molecular Biology, Bijenička 54, 10000 Zagreb, Croatia
(E-mail: iweber@irb.hr)*

RECEIVED NOVEMBER 26, 2004; REVISED MARCH 25, 2005; ACCEPTED APRIL 5, 2005

Keywords
actin
cytoskeleton
cryofixation
electron microscopy
tomography

Disclosing undistorted spatial organization of the actin cytoskeleton with molecular resolution is fundamental for understanding the cellular ultrastructure. Whereas important insights into the architecture of microfilament networks have been gained by negative staining, critical point drying, and freeze-fracturing methods, it is cryoelectron tomography that provides, for the first time, a comprehensive three-dimensional view of the intact actin cytoskeleton *in situ*. In particular, topological relationships such as microfilament three-dimensional proximity, angles at filament branching points, and modes of microfilament interaction with the plasma membrane can be visualized with an unprecedented accuracy using this technique. Further improvements are expected to bring the resolution into the realm of 2–3 nm, where automatic pattern-recognition methods can be applied to identify actin-binding complexes. Combining cryoelectron tomography with ultra-fine immunolabeling and high-resolution fluorescence microscopy will make it possible to correlate structural data on the nanometer scale with molecular specificity and dynamical information.

INTRODUCTION

From the early days of application of electron microscopy to biological material, the principal concern has been how to preserve natively hydrated, fragile cellular structures under the conditions of high vacuum in the column of an electron microscope. A sequence of harsh treatments was gradually included in the standard procedure for specimen preparation, which consists of fixating, drying, embedding, and staining steps that inevitably induce distortions to cell and tissue specimens that are sometimes difficult to recognize. A lot of research effort has been invested into optimizing these procedures to preserve specific cellular

regions, organelles and structures. Besides, the usual sectioning procedures allow us to observe the structural details revealed on the surface of mechanically sliced sections, but not the full three-dimensional architecture of the cytoplasm on the nanometer scale. These limitations are especially aggravating when it comes to study the structure of the actin cytoskeleton, a structure distinguished by its physical fragility and profound three-dimensional complexity.

Only actin filaments that are tightly bundled and crosslinked by actin-associated proteins, like those assembled in stress fibers, are relatively resistant to the se-

* Dedicated to Professor Željko Kućan on the occasion of his 70th birthday.

Presented at the Congress of the Croatian Society of Biochemistry and Molecular Biology, HDBMB₂₀₀₄, Bjelolasica, Croatia, September 30 – October 2, 2004.

verity of postfixation, dehydration, and embedding required for thin-section electron microscopy.¹ Single filaments or more loosely interconnected filament networks, either purified or examined *in situ*, are very sensitive to these procedures. Meshworks of actin filaments found in lamellipodia are particularly sensitive and become damaged by osmium tetroxide fixation and distorted by dehydration.² Prominent sensitivity of actin meshworks probably explains why little filament organization has been detected in lamellipodia of embedded cells.³ This is in contrast to more resistant microtubules and intermediate filaments, whose relative stability is most likely a result of their higher mechanical rigidity. To obtain meaningful results at the ultrastructural level, the methods employed should minimize structural distortions as well as the loss of material belonging to the cytoskeleton. A handful of preparative methods that partially meet these requirements are currently in use for visualization of the actin cytoskeleton with the high-resolution electron microscopy in whole-mount specimens.

Negative staining as a contrasting method has strongly contributed to determination of the actin filament structure, to localization of associated molecules on its surface, and to resolution of their structure.⁴ The contrast-generating step in the negative staining method consists of drying a specimen in a heavy metal salt. Preparative procedures generally consist of extraction by a nonionic detergent, *e.g.*, Triton X-100, with simultaneous fixation in glutaraldehyde, followed by application of phalloidin, which has the important function of stabilizing actin filaments against distortion during staining. Using this general procedure, the organization of actin filaments in the lamellipodia of a variety of cells has been investigated.⁵ The advantage of the negative stain method is that it is simple and fast, and that it preserves the straightness of the actin filaments within lamellipodium networks.

Air-drying of samples for electron microscopy leads to major distortions due to surface tension effects, which are avoided in the critical point drying method. Initial application of the critical point method to the actin cytoskeleton resulted in filaments of irregular outline and thickness, and induced their aggregation and distortion.⁶ Recent modifications of the procedure that include improving the contrast by metal coating after critical point drying and post-treatment of glutaraldehyde-fixed cytoskeletons with tannic acid and uranyl acetate, which presumably reduce distortions caused by dehydration, have led to a marked improvement in filament clarity and order. This procedure has been utilized with great success for immunoelectron microscopy with antibodies directed against several actin-binding proteins coupled to gold particles.⁷ It has also been successfully employed for correlated immunofluorescence and electron microscopy.⁸ The critical point drying technique requires detergent extraction without simultaneous fixation to ensure that

all surface membrane is removed, as well as dehydration in organic solvents, which may contribute to distortions. In addition, use of metal shadowing restricts the visibility of actin structures to the dorsal cell surface.

The quick-freeze deep-etch method, which has been successfully applied to visualize sub-membranous structures,⁹ is not equally suited for actin cytoskeletons of substrate-attached cells. The method relies on rapid freezing, and vitreous ice is subsequently sublimed at low temperature to expose the upper layers of the cytoplasm, which are then shadowed with platinum. The preservation of actin filament order in stress fibers and lamellipodia of cultured cell cytoskeletons does not match that achieved by either negative staining or critical point drying.¹⁰ This method does not offer the possibility of correlated light and electron microscopy of the same cells.

Taken together, the established methods for the preparation and visualization of the actin cytoskeleton by electron microscopy suffer from two major limitations. A certain amount of intervention by chemical and physical means is needed to arrest and preserve the specimen, as well as to enhance the contrast and improve the visibility of actin filaments. Also, conventional transmission electron microscopy provides orthogonal projections through the specimen, whereas reflection electron microscopy reveals the surface relief. In both cases, deep three-dimensional organization of the specimen remains concealed. The technique of cryoelectron tomography circumvents exactly these two limitations, which makes it perfectly suited for revelation of the precise three-dimensional structure of the actin cytoskeleton in its native state. First, tomographic imaging in an electron microscope enables spatial reconstruction of filamentous networks with a nanometer precision. Second, cryogenic preservation of native, unfixed, and fully hydrated biological material guarantees authenticity of the exposed structures.

CRYOELECTRON TOMOGRAPHY

Tomography involves regenerating a three-dimensional density distribution by combining a collection of two-dimensional projections of the three-dimensional object of interest. Tomographic imaging of human patients by X-ray radiation was introduced as a diagnostic method under the name of computer tomography (CT). Unlike radiological tomography, in which the patient remains static whereas source and detector are rotated, in electron tomography the microscope and camera remain fixed and the specimen is tilted in small steps through a predefined angular range. Three-dimensional electron density distribution is then calculated from the tilt series using a weighted back-projection algorithm. Resolution R of a tomographic reconstruction of an object that has a thickness T , from the number of projections N , is restricted to

$R \approx \pi T / N$. Thus, to achieve a resolution of ≈ 5 nm with a 200 nm thick specimen, about 130 equally spaced projections are required, for instance, taken at angular increments of 1° in the range between -65° and $+65^\circ$. Physical constraints prevent covering the full span of angles, and the resulting »missing wedge« of data results in anisotropic resolution with the resolution in the z -direction being reduced by almost 50 %.

Collecting a tilt series while maintaining a constant level of defocus and keeping the specimen centered in the field of view presents a formidable technical challenge. It is only recently that automatic collection procedures have been developed, making use of computer-controlled electron microscopes equipped with eucentric cryo-tilt stages. Images are recorded digitally on large-area charge-coupled device cameras. The tilt series and, consequently, reconstructed tomograms contain imposing amounts of data. A series consisting of 130 frames recorded with a 16 megapixel ($4k \times 4k$) CCD camera, having a dynamical range of ≈ 4000 gray values (2 bytes per pixel), contains 4 gigabytes of data.

The second principal benefit of the cryoelectron tomography is its capability to preserve the native structure of a specimen. This can be only achieved if the specimen remains hydrated during electron microscopy, which is accomplished through a process of vitrification. The specimen is rapidly plunged into a cryogen so that water becomes immobilized in a liquid-like non-crystalline state. Transferred into a cryogenic specimen holder and kept at all times cold enough to prevent phase transition from amorphous to crystalline ice, the cell and its contents remain intact. However, such optimal preservation has its price: unfixed and unstained biological specimens embedded in amorphous ice exhibit little contrast in projection images. Several measures are invoked to improve contrast. One is to enhance the phase contrast effect by working at high values of defocus. Another is to use post-column, zero-loss energy filtering in order to get rid of the inelastically scattered electrons whose relative yield increases strongly with specimen thickness and which degrade the image by chromatic aberration. A further provision to facilitate observation of thicker specimens is to use accelerating voltages in the intermediate range, between 300 and 400 kV, to obtain increased penetration.

The key problem in cryoelectron tomography lies in reconciling two conflicting requirements. On the one hand, to obtain a high-resolution tomographic reconstruction, a tilt series has to be recorded that covers as wide an angular range as possible in as many small increments as possible. On the other hand, the electron dose has to be kept low in order to reduce radiation damage inflicted upon delicate vitrified specimens. Successful application of cryoelectron tomography relies on the principle of dose fractionation, where the total subcritical dose is divided over as many projections as required. However,

with the reduced electron illumination, the resulting projections become increasingly noisy, thereby degrading resolution. The total maximal tolerable dose for vitrified specimens maintained at liquid-nitrogen temperature is near $5000 \text{ e}^- / \text{nm}^2$, which in the end limits the resolution under these conditions to about 4 nm.¹¹

Cryoelectron tomography has been successfully applied to visualize isolated macromolecular complexes, viruses, organelles, and prokaryotic cells. A three-dimensional map of the thermosome, an archeal member of the group II chaperonins, was obtained using isolated particles embedded in vitreous ice.¹² Analogously, the pleomorphic three-dimensional structure of the herpes simplex virus was analyzed.¹³ Cryoelectron tomography of fully native, vitrified mitochondria isolated from *Neurospora crassa* contributed to a new view of their inner membrane morphology.¹⁴ A system consisting of T5 phages and liposomes containing the phage receptor FhuA was reconstituted to mimic the transfer of DNA during the phage infection. Tomographic analysis revealed conformational changes at the tip of the phage tail upon binding to its receptor.¹⁵ Because of their small dimension, prokaryotic cells are well suited to vitrification and tomographic analysis *in toto*. However, it turned out that the dense packing of cytoplasmic components in these cells hampers interpretation of the obtained tomograms.¹⁶ Exceptions are the distinct features such as the homogeneous surface protein layer, and crystalline protein inclusions. In addition to vitrified whole-mount specimens, electron tomography of thick sections has also contributed important insights into the organization of the Golgi apparatus and endoplasmic reticulum,¹⁷ and the centrosome.¹⁸

Recently, the first application of cryoelectron tomography to intact, vitrified eukaryotic cells was reported.¹⁹ *Dictyostelium discoideum* cells chosen for this pioneering study are rather flat ($\approx 1 \mu\text{m}$), and thus thin enough to obtain tomograms at a resolution of 5 to 6 nm. In cryotomograms, the membrane of the endoplasmic reticulum could be readily identified but its content was too densely crowded to allow detailed interpretation. Unexpectedly, the cytoplasm turned out to be significantly less crowded, and mainly occupied by relatively large and separate complexes, which facilitated interpretation of tomograms at the attained resolution and signal-to-noise ratio. A large number of ribosomes were identified based on their overall size, shape and high mass density. The ribosomes were either bound to membranes of the endoplasmic reticulum, free in the cytoplasm, or apparently associated with the cytoskeleton. Also, 26S proteasomes, particles of the characteristic »double dragon head« shape, were identified, whose reconstructed subtomograms yielded a structure that closely resembles detailed reconstruction of proteasomes isolated from *Xenopus* and obtained by averaging thousands of single particle projec-

tions.²⁰ By careful inspection of reconstituted cytoplasmic spaces, it was even possible to detect and model a hitherto unknown particle that has a fivefold symmetry.²¹

IMPLICATIONS FOR ACTIN CYTOSKELETON RESEARCH

Most attention in the tomographic analysis of *Dictyostelium* cytoplasm was focused on the actin cytoskeleton, especially in the cortical region.¹⁹ In that work, it was possible to reconstruct volume segments crowded with actin filaments and to trace individual actin filaments over lengths up to 500 nm (Figure 1). Using appropriate graphical programs, it was possible to interactively rotate and examine reconstructed tomograms, and also to zoom into particular regions for detailed inspection. Actin filaments can be distinguished from other cytoplasmic components based on their shape of straight, thin rods. In this way, it is possible to perform purification of the actin cytoskeleton *in silico* and focus attention onto its organization (Figure 2). Two aspects of this organization can be analyzed separately: global architecture of the microfilament networks in distinct cellular regions, and local structural details on the level of single filaments. The ultimate goal will be to correlate these two levels of organization in order to understand how local macromolecular interactions, identified on the basis of their structural fingerprints, affect the general architecture of the microfilament system.

In highly motile cells such as those of *Dictyostelium*, the actin system can be reorganized within seconds. Numerous processes play a role in this reorganization, in particular polymerization and depolymerization of individual filaments, bifurcation of elongating filaments, as

well as orthogonal cross-linking and parallel bundling of formed filaments. These processes are under the control of dozens of actin-binding proteins and protein complexes, whose repertoire is similar in *Dictyostelium* to that in neutrophils and other fast moving animal cells.²² Of particular importance are the sites where actin filaments make contacts with the cell plasma membrane, because actin-membrane interactions directly influence changes of the cell shape. Very little is known about structural aspects of these interactions since most protocols for electron microscopy of whole cells include extraction of the plasma membrane.

It is quite obvious that a dynamical system such as the actin cytoskeleton will be especially sensitive to any treatment that perturbs the delicate balance of physical conditions and chemical factors in the cell, even for very short time intervals. In particular, dynamic equilibrium of various actin-binding proteins has to be preserved if a snapshot obtained by electron microscopy aspires to present the genuine, native situation. Also, osmotic shock and mechanical forces unleashed by standard preparative treatments lead to breakage, flattening and shrinkage of the actin network. Vitrification of thin aqueous layers occurs within milliseconds, and is probably the closest one can get to an »uninvasive« preservation of the cytoplasm.

Microfilament networks extracted from reconstructed tomograms leave an impression of overall heterogeneity. Whereas some regions are densely packed with filaments, others contain only a few long filaments (Figure 1). There is also a prominent local variability in directedness; in some cytoplasmic regions filaments are directed more or less parallel to each other, and in others they leave an impression of strong anisotropy.¹⁹ It has been estimated that the average volume fraction of the cytoplasm occupied by actin filaments makes up approximately 6 %. Single microfilaments appear to be quite straight, even the longest filaments exhibiting only slight curvature. It would be of interest to formulate numerical isotropy measures, three-dimensional order parameters for assemblies of thin rods, to quantitatively describe the local organization of the actin cytoskeleton and its variability.

Besides density and orientational order, connectivity is another principal characteristic of the microfilament network. Many actin-binding proteins are known to be specifically involved in creating links between actin filaments and connecting them either at an angle to each other (cross-linking) or in parallel orientation (bundling). At the present resolution of 5 to 6 nm, it is sometimes difficult to decide whether two closely apposed actin filaments, having a diameter of 8 to 9 nm, are actually attached to each other or not. This is an instance where improvement in resolution would open a possibility for automatic analysis of network connectivity.

Analysis of angles at which actin filaments intersect each other or bifurcate can also serve as a network des-

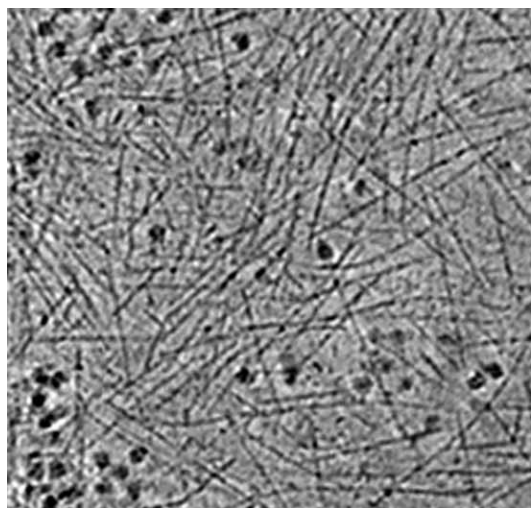


Figure 1. Cortical region of a vitrified *Dictyostelium* cell visualized by cryoelectron tomography (adapted from Ref. 19). A 60 nm thick slice through the tomogram near the ventral cell surface is shown. Numerous actin filaments and several ribosomes are visible.

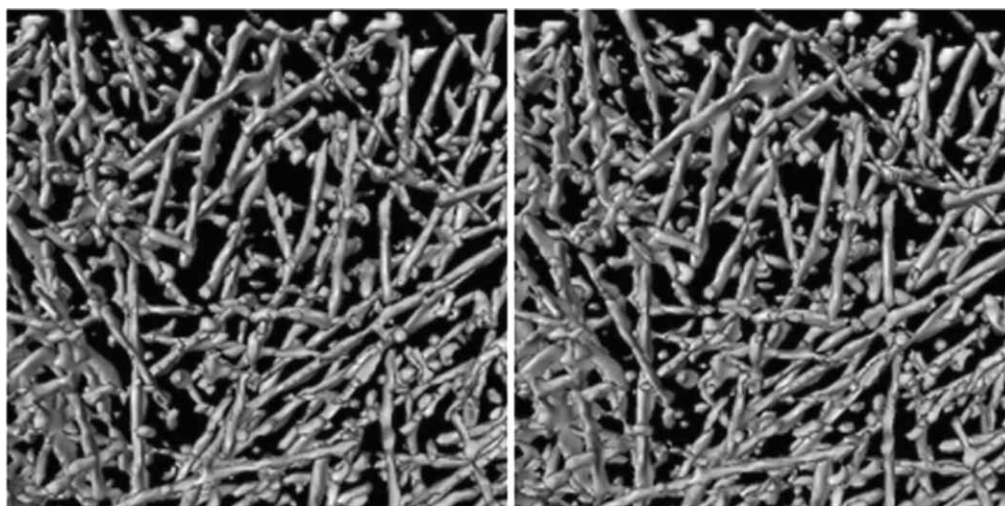


Figure 2. Surface-rendered view over a dense region of the actin cytoskeleton extracted from the tomogram shown in Figure 1 (adapted from Ref. 19). This stereo image displays a crowded isotropic network of branched and crosslinked microfilaments.

criptor (Figure 3). A characteristic range of angles is associated with each protein that crosslinks filaments or induces filament bifurcation. For instance, whereas the Arp 2/3 complex initiates new filaments that branch off the edges of the old filaments at a nearly fixed angle of 70° ,²³ α -actinin mediates a wide range of intersection angles due to flexible conformation of its rod domain.²⁴ At the present resolution, it should be possible to identify actin-crosslinking proteins of the spectrin family according to their shape and length. Elongated proteins like α -actinin, ABP-120, and filamin measure several dozens of nanometers in extended conformation and their atomic structures have been determined.^{24,25} In order to detect smaller and more compact proteins, such as the Arp 2/3 complex and fimbrin that extend only 10 to 15 nm in the largest dimension,^{23,26} improvement in resolution to 2–3 nm will probably be necessary.

The most promising strategy to positively identify proteins bound to actin filaments *in situ* would be to dock an atomic structure of F-actin to filaments extracted from tomograms.²⁷ The residual electron density can then be

searched for characteristic structural signatures of actin-binding proteins, applying *e.g.* template-searching algorithms already utilized to identify complexes larger than ≈ 400 kDa in tomograms.²⁸ Another approach to specifying molecular composition of the actin cytoskeleton in intact cells would be to combine cryoelectron tomography with immunolabeling by specific antibodies conjugated to ultrasmall gold particles, which are able to enter cells without removal of the plasma membrane.²⁹ It is probably the combination of the two complementary approaches, structural template-matching and immunolabeling, that will prove to be most informative.

A truly unique advantage of the cryoelectron tomography is its capability to visualize sites where actin filaments closely approach, or attach to cellular membranes (Figure 4). Two types of filament-membrane interaction can be distinguished: lateral and end-on attachment.¹⁹ The structure of the latter is of particular importance, because of its relevance to the mechanism of membrane protrusion induced by actin polymerization.³⁰ The presence or absence of certain proteins at the sites of filament-membrane contact can offer decisive arguments for any of the alternative models of cell motility. Cryoelectron tomography opens up an exclusive possibility to analyze integral membrane complexes that anchor actin filaments, like focal and tight junction complexes, in their unperturbed natural milieu. Presently, the main obstacle to disclose structural details at the membrane-microfilament interface is anisotropic resolution of tomograms obtained from tilt series collected using single-axis goniometers. Most of the plasma membrane area in thin cell regions is oriented perpendicularly to the tilting plane, and resolution of membrane components in the longitudinal direction suffers most from the missing wedge effect. Use of the double-axis goniometers will significantly reduce this deficiency.

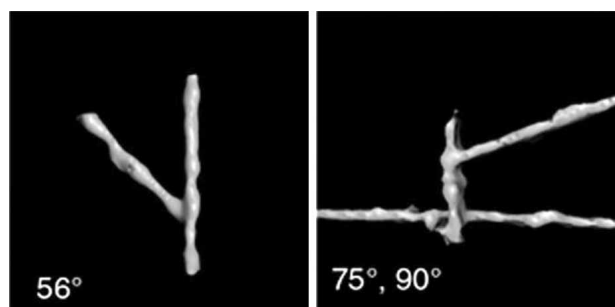


Figure 3. Two examples of branches and cross-linkages between actin filaments extracted from the surface-rendered tomograms similar to that shown in Figure 2 (adapted from Ref. 19). Angles were isolated from three-dimensional reconstructions, and their maximal projections are displayed in two dimensions.

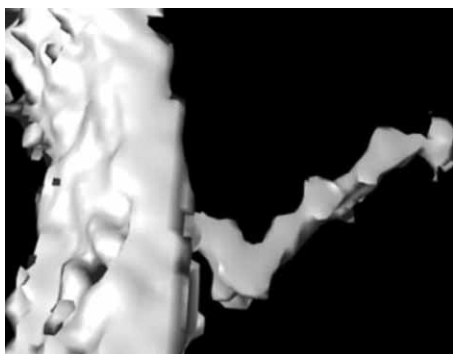


Figure 4. Visualization of the end-on contact of an actin filament to the plasma membrane (adapted from Ref. 19). Filament appears to be attached to the membrane through a kink-like structure.

CONCLUDING REMARKS

Cryoelectron tomography provides a means for visualizing the actin cytoskeleton in an unperturbed cellular context and for analyzing it at the level of individual filaments. In essence, cryotomograms obtained at molecular resolution represent three-dimensional images of the cell's entire proteome, from which a subset containing the actin cytoskeleton can be extracted by image-processing methods. Resolution in tomograms of suitably thin specimens, currently 5 to 6 nm, can be improved by using more projections with smaller angular increments while collecting a tilt series. To counter the ensuing radiation damage, liquid-helium-cooled specimen holders will have to be used. In addition to implementation of sophisticated denoising algorithms, noise can be suppressed by the use of detectors optimized for intermediate voltage transmission electron microscopes, and contrast can be enhanced by similar improvements in electron optics. The drop of resolution in the dimension along the optical axis can be reduced by application of dual-axis tilting devices. Altogether, prospects for more isotropic resolution near 2 nm to be attained are good.

For thicker specimens, more projections are required for the same nominal resolution, and use of higher accelerating voltages in conjunction with working at liquid helium temperatures offers some improvement. However, to explore large cells, multicellular organisms and tissues in a vitrified state, reliable protocols will have to be developed for sectioning frozen-hydrated material, whereby vitrification of thick specimens can be accomplished by high-pressure freezing.³¹ Influence of these, still experimental, procedures on the structural integrity of the actin cytoskeleton have yet to be determined. Also, correlative light and electron microscopy techniques are required, which would make it possible to associate certain structural microfilament arrangements with specific physiological states and dynamic activities in the cell cortex.³²

REFERENCES

1. L. G. Tilney, P. S. Connelly, L. Ruggiero, K. A. Vranich, and G. M. Guild, *Mol. Biol. Cell* **74** (2003) 3953–3966.
2. J. V. Small, *J. Cell Biol.* **91** (1981) 695–705.
3. J. P. Heath and G. A. Dunn, *J. Cell Sci.* **29** (1978) 197–212.
4. M. O. Steinmetz, D. Stoffler, A. Hoenger, A. Bremer, and U. Aebi, *J. Struct. Biol.* **119** (1997) 295–320.
5. J. V. Small, K. Rottner, P. Hahne, and K. I. Anderson, *Microsc. Res. Technique* **47** (1999) 3–17.
6. J. V. Small, *Electron Microsc. Rev.* **1** (1988) 155–174.
7. T. M. Svitkina, E. A. Bulanova, O. Y. Chaga, D. M. Vignjevic, S. Kojima, J. M. Vasiliev, and G. G. Borisy, *J. Cell Biol.* **160** (2003) 409–421.
8. T. M. Svitkina and G. G. Borisy, *J. Cell Biol.* **145** (1999) 1009–1026.
9. J. Heuser, *Traffic* **1** (2000) 545–552.
10. J. E. Heuser and M. W. Kirschner, *J. Cell Biol.* **86** (1980) 212–234.
11. R. Henderson, *Q. Rev. Biophys.* **37** (2004) 3–13.
12. M. Nitsch, J. Walz, D. Typke, M. Klumpp, L. O. Essen, and W. Baumeister, *Nat. Struct. Biol.* **5** (1998) 855–857.
13. K. Grünwald, P. Desai, D. C. Winkler, J. B. Heymann, D. M. Belnap, W. Baumeister, and A. C. Steven, *Science* **302** (2003) 1396–1398.
14. D. Nicastro, A. S. Frangakis, D. Typke, and W. Baumeister, *J. Struct. Biol.* **129** (2000) 48–56.
15. J. Böhm, O. Lambert, A. S. Frangakis, L. Letellier, W. Baumeister, and J. L. Rigaud, *Curr. Biol.* **11** (2001) 1168–1175.
16. R. Grimm, H. Singh, R. Rachel, D. Typke, W. Zillig, and W. Baumeister, *Biophys. J.* **74** (1998) 1031–1042.
17. S. Mogelsvang, B. J. Marsh, M. S. Ladinsky, and K. E. Howell, *Traffic* **5** (2004) 338–345.
18. J. R. McIntosh, *J. Cell Biol.* **153** (2001) F25–F32.
19. O. Medalia, I. Weber, A. S. Frangakis, D. Nicastro, G. Gerisch, and W. Baumeister, *Science* **298** (2002) 1209–1213.
20. J. Walz, A. Erdmann, M. Kania, D. Typke, A. J. Koster, and W. Baumeister, *J. Struct. Biol.* **121** (1998) 19–29.
21. K. Grünwald, O. Medalia, A. Gross, A. C. Steven, and W. Baumeister, *Biophys. Chem.* **100** (2003) 577–591.
22. I. Weber, *Recent Res. Dev. Mol. Cell. Biol.* **4** (2003) 273–295.
23. N. Volkmann, K. J. Amann, S. Stoilova-McPhie, C. Egile, D. C. Winter, L. Hazelwood, J. E. Heuser, R. Li, T. D. Pollard, and D. Hanein, *Science* **293** (2001) 2456–2459.
24. J. Tang, D. W. Taylor, and K. A. Taylor, *J. Mol. Biol.* **310** (2001) 845–858.
25. G. M. Popowicz, R. Muller, A. A. Noegel, M. Schleicher, R. Huber, and T. A. Holak, *J. Mol. Biol.* **342** (2004) 1637–46.
26. N. Volkmann, D. DeRosier, P. Matsudaira, and D. Hanein, *J. Cell Biol.* **153** (2001) 947–956.
27. J. Kürner, O. Medalia, A. A. Linaroudis, and W. Baumeister, *Exp. Cell Res.* **301** (2004) 38–42.
28. A. S. Frangakis, J. Böhm, F. Förster, S. Nickell, D. Nicastro, D. Typke, R. Hegerl, and W. Baumeister, *Proc. Natl. Acad. Sci. USA* **99** (2002) 14153–14158.
29. U. Ziese, C. Kubel, A. J. Verkleij, and A. J. Koster, *J. Struct. Biol.* **138** (2002) 58–62.
30. J. A. Theriot, *Traffic* **1** (2000) 19–28.
31. P. Walther, *J. Microsc.* **212** (2003) 34–43.
32. T. Bretschneider, J. Jonkman, J. Köhler, O. Medalia, K. Barisic, I. Weber, E. H. K. Stelzer, W. Baumeister, and G. Gerisch, *J. Muscle Res. Cell Motil.* **23** (2002) 639–649.

SAŽETAK

Krioelektronska tomografija: implikacije za istraživanje aktinskoga citoskeleta

Igor Weber

Razotkrivanje netaknute prostorne organizacije aktinskoga citoskeleta na molekularnoj razini od temeljne je važnosti za razumijevanje stanične ultrastrukture. Iako su tehnike negativnoga bojanja, sušenja na kritičnoj točki i kalanja smrznutih uzoraka omogućile značajne uvide u arhitekturu umrežavanja mikrofilamenata, tek je krioelektronska tomografija po prvi puta otvorila sveobuhvatni trodimenzionalni vidik na intaktni aktinski citoskelet *in situ*. Posebice, topološki odnosi poput međusobnoga položaja mikrofilamenata u prostoru, kutova grananja filamenata, kao i načina interakcije filamenata sa staničnom membranom mogu biti predloženi pomoću ove tehnike s do sada nedosegnutom točnošću. Očekuje se daljnje poboljšanje moći razlučivanja do područja između 2 i 3 nm, kada će biti moguće primijeniti automatske metode prepoznavanja uzoraka za identifikaciju kompleksa vezanih uz aktin. Kombiniranje krioelektronske tomografije s ultrafinim imunooznačavanjem i fluorescencijskom mikroskopijom velike rezolucije omogućit će korelaciju strukturnih podataka na nanometarskoj skali s molekularnom specifičnošću i dinamičkom informacijom.